Eddy Formation in Obstructed Fluid Flow: A Molecular-Dynamics Study

D. C. Rapaport[a] and E. Clementi
IBM Corporation, Kingston, New York 12401
(Received 28 May 1986)

Two-dimensional fluid flow past a circular obstacle has been simulated at the microscopic level by means of a molecular-dynamics approach. At sufficiently large Reynolds number the flow field is observed to exhibit characteristics common to real fluids, namely the appearance of eddies, periodic eddy separation, and an oscillatory wake. Very large systems—typically 160 000 particles—are required in order to provide adequate space for these flow patterns to develop.

PACS numbers: 47.10.+g, 47.15.Ki, 51.10.+y

The phenomena of eddy formation and shedding that occur in fluid flow past a cylindrical obstacle and their detailed dependence on the Reynolds number, N_{Re}, of the flow have been explored experimentally in considerable detail.[1,2] The initial departure from Stokes flow occurs at $N_{\mathrm{Re}} \simeq 5$, at which point a pair of counter-rotating eddies (or vortices) begins to develop at the downstream boundary of the cylinder. The eddies grow in size while at $N_{\mathrm{Re}} \simeq 34$ an oscillatory wake is seen in the flow downstream of the obstacle. At slightly higher N_{Re}, somewhere in the range 55–70, transverse oscillations begin to occur in the eddy structure accompanied by periodic shedding of rotating fluid regions, and the von Kármán vortex street makes its first appearance. Above $N_{\mathrm{Re}} \simeq 100$ the eddy structure immediately behind the cylinder ceases to be visible. There exists a considerable body of photographic documentation of these effects.[3,4] Similar low-N_{Re} behavior has also been seen in numerical solution of the equations of continuum hydrodynamics.[5] Cellular automata have recently been proposed as an alternative computational approach,[6] although the efficacy of the method has yet to be established.[7]

It is possible, in principle, to carry out detailed molecular-dynamics (MD) simulations of many-particle systems that are sufficiently large to allow generation of the flow instabilities that appear at nonzero Reynolds number. In this Letter we describe the results of an MD study of two-dimensional flow; the obstacle in this case is circular, the analog of a relatively long transverse cylinder in 3D flow experiments. While the MD technique has been used with great success in a wide variety of contexts to study both equilibrium and nonequilibrium behavior,[8,9] the difficulty in using it to study hydrodynamic instabilities lies in the size of system that must be dealt with computationally. The majority of MD calculations have employed systems with 10^2 to 10^4 particles; it turns out that, for reasons which will become apparent below, in order to attain even the lower range of N_{Re} values at which deviations from Stokes flow appear, considerably larger systems are required, typically containing more than 10^5 particles.

The MD simulation uses a purely repulsive short-range pair potential given by $V(r) = r^{-12} - r^{-6} + \frac{1}{4}$ for $r < r_c = 2^{1/6}$, and zero for $r > r_c$; the particles can be regarded as disks with an effective diameter close to unity. The circular obstacle has diameter D and is positioned at some suitable point in the flow (see Fig. 1); particles approaching the obstacle experience a repulsion given by $V(r - D/2)$, where $r(> D/2)$ is the distance from the center of the obstacle. The "collisions" with the obstacle are specular; in the language of hydrodynamics this corresponds to a slip boundary.[3] (The effect of nonslip boundaries can be emulated by replacement of the tangential velocity component at the instant of closest approach with an appropriate ran-

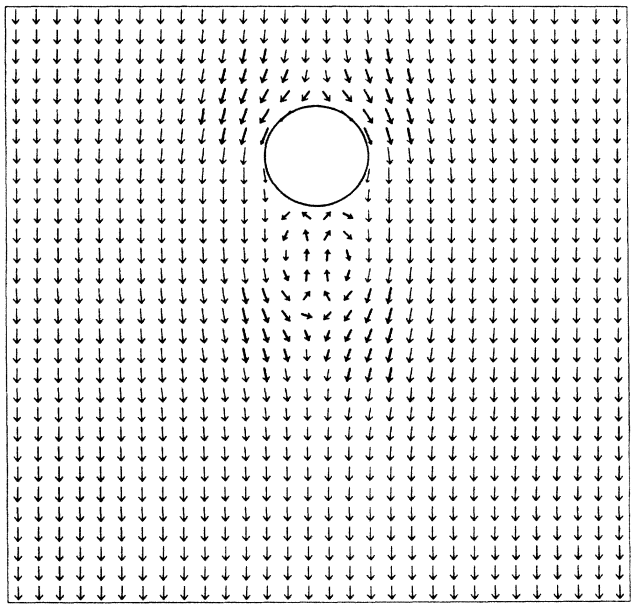

FIG. 1. The entire flow field at $t = 750$ showing the position of the eddy pair relative to the location of the circular obstacle. The flow is from top to bottom; thicker arrows are used where the local flow direction deviates significantly (by $> 10°$). Arrow length is related to local velocity; see text.

dom quantity having zero mean; this was not found to alter qualitatively the outcome of the simulations. Although nonslip boundaries are generally considered necessary for eddy formation, this was recently shown not to be the case.[10])

The boundaries of the region enclosing the fluid are periodic; when particles exit downstream they are reintroduced upstream with an initial flow velocity U_0 on which is superimposed an appropriate random thermal velocity. At the beginning of the simulation the entire system is given the same uniform flow velocity U_0, again with thermal motion superimposed. Finally, because collisions with the obstacle dissipate flow momentum, a gravitational field g is imposed in the appropriate direction to maintain the flow; its strength must be determined empirically in order to ensure the desired flow rate.

The particular calculations described here involve $(1.6\text{–}1.7)\times 10^5$ particles at a density $\rho = 0.83$ (particles/unit area), while the value of D is 74. If the unit of length is given its typical MD value,[11] namely 3.4 Å, then the simulation covers a square region of edge 1500 Å and the obstacle size is 250 Å. The unit of time is 0.31 psec; in terms of scaled units $U_0 = 0.3$ (on this scale the thermal velocity is 0.2 and the speed of sound 0.8) and $g = 2\times 10^{-4}$. The equations of motion are solved by use of a third-order predictor-corrector method with time step 0.03. The particular run described below extended over 1.2×10^5 steps corresponding to a total of 1.1 nsec; other runs briefly mentioned were of similar size and duration (unless stated otherwise).

One novel aspect of this simulation, apart from the comparatively large (by MD standards) size of the system, is the fact that the computations were carried out by use of a coupled array of four FPS 264 scientific processors.[12] The processors operate in parallel, each taking responsibility for a separate subregion of the system. A certain amount of data must be exchanged between the processors throughout the course of the calculation to allow for (i) motion of particles between adjacent subregions, and (ii) the evaluation of interactions for particles lying within a distance r_c of the subregion boundaries.

The results are summarized by introduction of a 60×60 grid that covers the entire system and, every fifth step, averaging of the properties of all the particles contained in each grid cell at that instant. The results described here represent the mean of either 400 or 1000 such sets of values, but no additional smoothing is applied to the data. The detailed evolution of the flow patterns depends on the initial conditions (a similar lack of reproducibility is observed in real fluids); we describe the principal features seen in one typical simulation run and briefly mention the changes observed in several other runs under altered conditions. At this stage the primary results of the simulations are descriptive in nature; space limitations permit the display of only a limited sampling of the flow patterns obtained.

The uniform flow at time $t = 0$ rapidly changed into Stokes flow around the obstacle. By $t \simeq 360$ a pair of counter-rotating eddies had developed adjacent to the downstream edge of the obstacle. The length of the recirculatory region grew steady, reaching approximately $1.4D$ at $t \simeq 850$. The time-averaged flow field at $t = 750$ (an average over 1000 configurations from the preceding interval of length $\Delta t = 150$) is shown in Fig. 1; the grid is 30×30 with each cell representing an average of 4 cells of the original grid, while the arrow length is a measure of the averaged local velocity v via the relation *length* $\propto 1 + v/v_{\max}$, and the arrow direction is that of the local flow. A more detailed illustration of the flow pattern appears in Fig. 2 where only the central 30×30 (original) grid cells are shown; the flow separation from the obstacle boundary is clearly visible, as are the flows within the eddies. The backflow velocity amounts to only about 10% of the overall flow speed; the compressible nature of the fluid is manifested most strongly just downstream of the obstacle where a 25% density drop occurs.

The next qualitative change that occurs is the breakdown of the bilateral symmetry of the flow—the counterclockwise (left) eddy begins to grow at the expense of the clockwise (right) eddy, the latter effectively disappearing at $t \simeq 1000$. The symmetry is restored by $t \simeq 1200$, but at $t \simeq 1500$ only the clockwise eddy is seen. This in turn separates from the obstacle and the

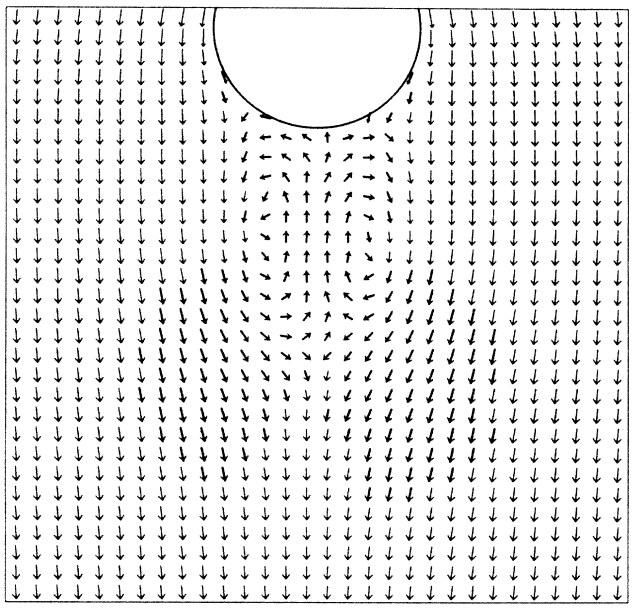

FIG. 2. Enlarged central region of Fig. 1 showing the flow pattern in and around the eddies.

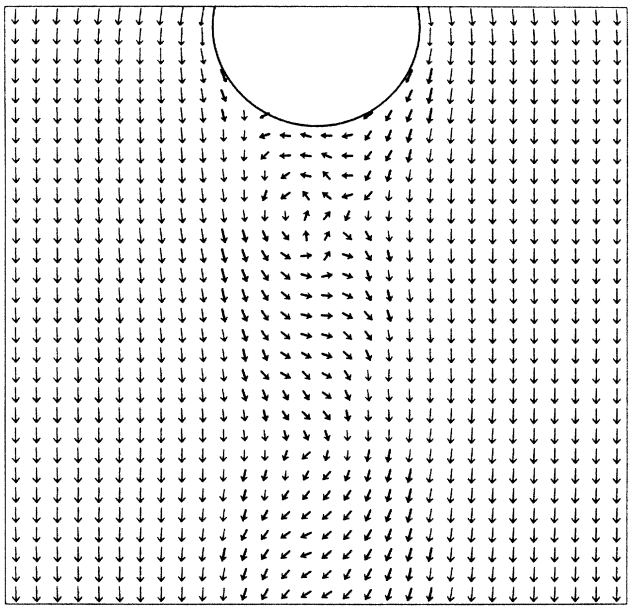

FIG. 3. Central region of system at $t = 2400$ showing the single eddy that is present and a portion of the oscillatory wake.

opposite eddy develops. Alternate eddy formation and shedding is repeated several times and an oscillatory wake develops at $t \simeq 2000$. Figure 3 shows the central portion of the flow field at $t \simeq 2400$; the wake—a remnant of previously shed eddies—is clearly visible, as is a counterclockwise eddy still attached to the obstacle. By $t \simeq 2700$ the transverse flow component has reversed itself, and the flow pattern is essentially the mirror image of Fig. 3. While the wake oscillations continue until (and presumably beyond) the end of the run ($t = 3600$), the recirculation that characterizes the eddies eventually vanishes and the sinuous wake is found to extend right up to the obstacle.

The Reynolds number[3] is defined as $N_{\mathrm{Re}} = DU/\nu$, where U is the flow velocity and ν the kinematic viscosity. The average flow velocity is approximately 0.4 (reached at $t \simeq 1800$); since $\nu = \mu/\rho$, and the shear viscosity μ is available from earlier 2D simulation,[13] we obtain $N_{\mathrm{Re}} \simeq 25$. This estimate of N_{Re} is only a rough one since there is arbitrariness in the choice of U and, in 2D, μ exhibits a complex dependence on both the shear rate and the extent of the sheared region[11,13]; nevertheless, it does suggest that the MD fluid is flowing with a value of N_{Re} in the range at which eddy formation is observed experimentally. Further simulation over a range of N_{Re} would be required to establish whether stationary eddy formation is possible on the length scales accessible to MD.

A partial history of the wake is shown in Fig. 4. Each frame of the sequence represents an average over an interval $\Delta t = 60$ (corresponding to 400 configurations) and shows the flow in the central downstream portion of the system covered by a 20×40 section of the grid. The propagating waveform is clearly visible. The dimensionless number associated with wake oscillation is the Strouhal number $N_{\mathrm{Sr}} = fD/U$, where f is the oscillation frequency.[1,3] The value of f is obtained by direct measurement of the oscillation wavelength ($\simeq 220$ in scaled units) and group velocity ($\simeq 0.24$ —a value significantly lower than the flow speed) from plots similar to those in Fig. 4. The result is $N_{\mathrm{Sr}} \simeq 0.2$, an estimate not too different from the experimental 0.15 measured at low N_{Re},[1] or a similar value obtained by numerical solution of the Navier-Stokes equations.[5]

Behavior qualitatively similar to that just described was observed in another MD run in which the average flow velocity was reduced by 10%. On the other hand, when the flow speed was reduced by 50% there was only the slightest hint of deviation from Stokes flow (run duration 0.7 nsec); this is evidence for the existence of a critical Reynolds number $N_{\mathrm{Re},c} > 0$ for the onset of eddy formation. In yet another run, for which

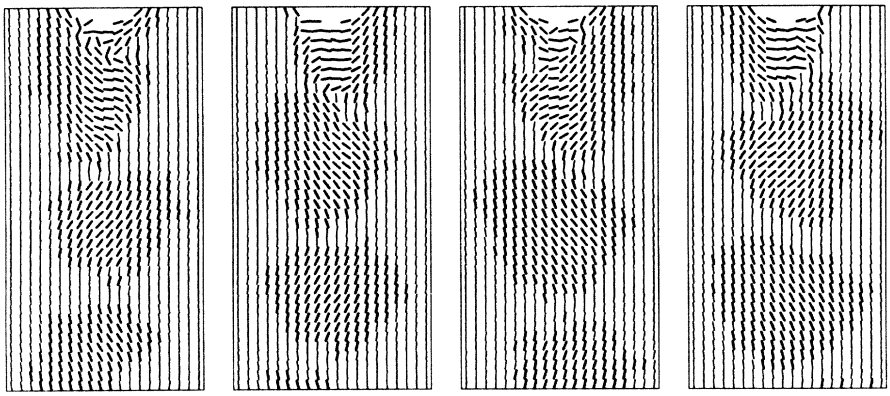

FIG. 4. Flow fields (direction only) at a series of evenly spaced intervals between $t = 3000$ and 3540; the development and propagation of wake oscillations can be seen. An observer moving with the wake will see a vortex street.

the velocity was 25% greater, the eddies stretched almost to the downstream boundary of the system before any oscillation became apparent; clearly the limited system size had a pronounced influence on the flow development in this particular instance.

The need for comparatively large numbers of particles—the present work involves some of the largest MD simulations carried out to date—is a consequence of the requirement that $N_{\mathrm{Re}} > N_{\mathrm{Re},c}$. Since the flow should be kept subsonic to avoid possible shock waves, N_{Re} can only be increased by enlarging of the obstacle; this implies the need for a larger region, and therefore an increased number of particles in order to maintain a similar density. The reason for this is that the obstacle must be kept small relative to the linear dimensions of the region, both to avoid excessive velocity gradients and to allow adequate space for flow patterns to develop.

An alternative method of enlarging the system is to reduce ρ. One such run was carried out with 40 000 particles at a density $\frac{1}{16}$ of the value used above and with an obstacle having double the diameter. No deviation from Stokes flow was observed, suggesting a lower effective N_{Re} than before. This is not unexpected, since at sufficiently low ρ, $\nu \propto \lambda$—the mean free path—and therefore $N_{\mathrm{Re}} \propto 1/\lambda$; furthermore, deviations from hydrodynamics can be expected as λ/D—the Knudsen number—increases from the fluid value of 10^{-3}.

There has been one other MD study that attempted to observe the appearance of eddies in fluid flow past an obstacle.[14] Eddies were seen shedding from the tips of a thin inclined plate, but since $N_{\mathrm{Re},c}$ decreases with increasing curvature of the side of the obstacle, the sharp tip implies $N_{\mathrm{Re},c} = 0$,[3] and therefore eddy formation is to be expected even at arbitrarily small N_{Re} (although the shedding suggests a larger N_{Re}). The one key difference between a gently curved obstacle boundary and one with sharp corners is that, in the former, flow separation occurs at a stagnation point[3] whose position depends on N_{Re}, whereas in the latter, separation occurs at the sharp corner itself since the flow cannot follow the abrupt changes in boundary direction.

The results obtained in the present study suggest that the MD approach may prove to be a valuable tool for probing of the detailed microscopic flow structures that underlie certain instabilities of continuum hydrodynamics. There are, of course, severe limitations as to the length and time scales that can be handled, as well as to the opportunities for similar work in 3D, and the exploration of phenomena such as turbulence appears to lie beyond the scope of detailed MD simulation. The gradients present in the MD simulations are much larger than those encountered in normal hydrodynamic situations, and on these grounds it is reasonable to believe that, at best, only qualitative agreement between MD and hydrodynamics might be found. Even at this level of expectation, however, the observed similarity between the flow patterns of MD and real fluids is quite remarkable.

We thank L. Hannon, G. Lie, V. Sonnad, and V. Yakhot for useful discussion.

---

[a]Permanent address: Department of Physics, Bar-Ilan University, Ramat-Gan, Israel.

[1]J. H. Gerrard, Philos. Trans. Roy. Soc. London, Ser. A **288**, 351 (1978).

[2]A. E. Perry, M. S. Chong, and T. T. Lim, J. Fluid Mech. **116**, 77 (1982).

[3]G. K. Batchelor, *An Introduction to Fluid Dynamics* (Cambridge Univ. Press, Cambridge, United Kingdom, 1967).

[4]M. van Dyke, *An Album of Fluid Motion* (Parabolic, Stanford, CA, 1982).

[5]S. K. Jordan and J. E. Fromm, Phys. Fluids **15**, 371 (1972).

[6]U. Frisch, B. Hasslacher, and Y. Pomeau, Phys. Rev Lett. **56**, 1505 (1986); N. Margolis, T. Toffoli, and G. Vichniac, Phys. Rev. Lett. **56**, 1694 (1986); J. B. Salem and S. Wolfram, Thinking Machines Corporation Technical Report No. 86.14, 1986 (unpublished).

[7]S. A. Orszag and V. Yakhot, Phys. Rev. Lett. **56**, 1691 (1986).

[8]D. J. Evans and W. G. Hoover, Annu. Rev. Fluid Mech. **18**, 243 (1986).

[9]"Molecular Dynamics Simulation of Statistical Mechanical Systems," edited by G. Ciccotti and W. G. Hoover, International School of Physics "Enrico Fermi," Course 97 (North-Holland, Amsterdam, to be published).

[10]D. S. Dandy and L. G. Leal, Phys. Fluids **29**, 1360 (1986).

[11]W. G. Hoover and W. T. Ashurst, in *Theoretical Chemistry, Advances and Perspectives,* edited by H. Eyring and D. Henderson (Academic, New York, 1975), Vol. 1, p. 1.

[12]E. Clementi, G. Corongiu, and J. H. Detrich, Comput. Phys. Commun. **37**, 287 (1985); E. Clementi and D. Logan, IBM Report No. KGN-43, 1985 (unpublished).

[13]D. M. Heyes, G. P. Morriss, and D. J. Evans, J. Chem. Phys. **83**, 4760 (1985).

[14]E. Meiburg, Deutschen Forschungs- und Versuchsanstalt für Luft- und Raumfahrt (DFVLR) Report No. FB85-13, 1985 (unpublished); see also Ref. 8.